arXiv:1112.5400v2 [cond-mat.mes-hall] 29 Jun 2012

Magnetic field induced Fabry-Pérot resonances in helical edge states

Abhiram Soori[1], Sourin Das[2] and Sumathi Rao[3]
[1] *Centre for High Energy Physics, Indian Institute of Science, Bangalore 560012, India.*
[2] *Department of Physics and Astrophysics, University of Delhi, Delhi - 110 007, India.*
[3] *Harish-Chandra Research Institute, Chhatnag Road, Jhusi, Allahabad 211 019, India.*

We study electronic transport across a helical edge state exposed to a uniform magnetic ($\vec{B}$) field over a finite length. We show that this system exhibits Fabry-Pérot type resonances in electronic transport. The intrinsic spin anisotropy of the helical edge states allows us to tune these resonances by changing the direction of the $\vec{B}$ field while keeping its magnitude constant. This is in sharp contrast to the case of non-helical one dimensional electron gases with a parabolic dispersion, where similar resonances do appear in individual spin channels (↑ and ↓) separately which, however, cannot be tuned by merely changing the direction of the $\vec{B}$ field. These resonances provide a unique way to probe the helical nature of the theory.

PACS numbers: 73.23.-b, 73.63.Nm, 71.10.Pm

Introduction :- Edge states of a new class of insulators called topological insulators form an interesting class of 1-D systems called helical edge states (HES)[1]. The central feature of these edge states is the fact that the direction of propagation of the quasi-particles is directly correlated with their spin projection, i.e., counter-propagating particles have opposite spin projections. Various aspects of this state have been studied[2]. Experimental evidence has been found for the existence of these edge states in a multi-terminal Hall bar setup[3].

The fact that the spin of the electrons can be controlled and manipulated by manipulating its momentum due to spin-momentum locking has generated great interest in the possible application of HES to the field of spintronics[4]. Besides electrical control, it is interesting to study the possibility of controlling the spin of electrons on such edge states using magnetic fields. This could be of great interest from the point of view of application to spintronics devices. Since spin rotation symmetry is strongly broken in such edge states, a strong anisotropic response to an applied magnetic field is expected, which, in turn could be exploited for various applications. Hence one of the more intriguing features of the HES as opposed to the usual one dimensional electron gas with parabolic dispersion lies in its response to magnetic fields. Naively, the introduction of a magnetic field breaks the time-reversal symmetry which is central to the topological stability of the quantum Hall insulators which hosts these HES on its boundary. However, it is still of interest to study the response of the HES to small magnetic fields which do not significantly disturb the bulk stability of the topological insulators but do influence the edge states in a nontrivial way.

From the viewpoint of device-applications, the study of tunneling across barriers or back scattering from tunnel barriers implanted on the edge states is of central interest as they can act as experimentally tunable quantum resistors which are essential elements of any quantum circuitry. A simple way to produce controlled backscattering in mesoscopic devices is to apply local gate voltages. But for HES such techniques are not effective because all electrical barriers are rendered transparent due to Klein tunneling of massless Dirac electrons. Further, protection of HES against inelastic backscattering due to electron-phonon coupling has also been reported [5]. Hence, an alternate way is needed to produce back-scattering, and therefore, magnetic barriers which do give rise to back-scattering are of vital importance in the context of HES. One of the more interesting aspects which has not yet been explored in this context is the fact that the effective size of the barrier depends also on the direction of the applied $\vec{B}$-field and not just its magnitude. Transmission through magnetic barriers has been studied in the case of chiral modes in carbon nanotubes [6] and surface states of 3-D topological insulators [7]; however, a similar study for HES is lacking and such a study is the central focus of this letter. Also, recently there have been theoretical studies involving spin-polarised STM as a direct probe for testing the theoretical prediction of the helical nature of the surface states, both in the context of 2-D and 3-D topological insulators [8]. Experimentally, only very recently[9] the spin polarization at the edge was studied purely by electrical means; hence such proposals are of crucial importance. This letter provides yet another way to probe the helical nature of HES via the study of spin anisotropy driven Fabry-Pérot type resonances.

In this letter, we study the effect of a magnetic field patch on edge-state transport. We find that any $\vec{B}$-field with a non-zero component in the plane perpendicular to the spin quantization axis of left and right moving states opens up a gap in the spectrum. Further, the spin of the left and right moving states gets twisted. In other words, even in the presence of the $\vec{B}$-field, the direction of motion remains tied with its spin; however, unlike in free HES, the counter-propagating states no longer have spins anti-parallel to each other. We show that these states in the $\vec{B}$-field patch induce Fabry-Pérot type resonances in transport across the patch which are tunable purely by tuning the direction of the $\vec{B}$-field. The resonances, hence, provide a direct way to quantify the degree of spin anisotropy in these systems.

The model :- We consider a situation where an infinitely extended helical edge state is exposed to a uniform $\vec{B}$-field over a finite length L. As long as the edge is smooth, the free edge can be described by a Hamiltonian given below [1]

$$H_0 = -i\hbar v_F \int dx\ \psi^\dagger(x)\sigma_z \partial_x \psi(x)\ , \qquad (1)$$

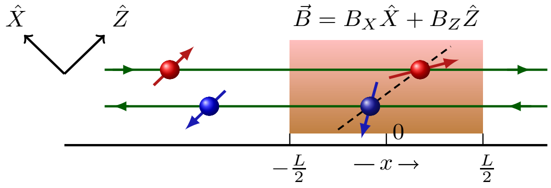

FIG. 1. Schematic of the model. Shaded region $|x| < L/2$ is the region of constant magnetic field $\vec{B}$. Spin orientations of the left (right)-moving modes are tilted by B_X in clock (anti-clock)-wise direction by the same angle.

where $\psi = [\psi_{R\uparrow}\ \psi_{L\downarrow}]^T$ and the R/L index corresponds to right and left movers. Note that here we have used x to parametrize the coordinate along the 1-D edge state. X, Y, Z are chosen to describe the spin in such a way that Z points along the spin quantization axis of right-moving eigenstates in absence of $\vec{B}$ field. We choose X to be along the component of applied $\vec{B}$ in the plane perpendicular to Z. Since the spin and the direction of propagation are correlated in a HES, we will henceforth drop the L/R -indices in $\psi_{L/R\ \sigma}$. We now introduce a uniform magnetic field in the region $|x| < L/2$ (sketched in Fig. 1). The Zeeman coupling of the magnetic field to the intrinsic spin of the electrons can be modeled by

$$H_B = g\mu_B \int dx\ \Delta_L(x)\vec{S}(x)\cdot\vec{B}\ , \qquad (2)$$

where $\Delta_L(x) = [\Theta(x+L/2) - \Theta(x-L/2)]$, $\vec{S}(x) = 1/2(\psi^\dagger(x)\,\vec{\sigma}\,\psi(x))$ is the spin operator, g is the g-factor of the electron and μ_B is the Bohr magneton. The corresponding Heisenberg equations of motion for the fields $\psi(x,t)$ is given by

$$i\hbar\partial_t\psi = [-i\hbar v_F\sigma_z\partial_x + \frac{g}{2}\mu_B\Delta_L(x)\vec{\sigma}\cdot\vec{B}]\psi \qquad (3)$$

By rescaling the energy $E \rightarrow E/W$, and by defining the dimensionless variables $x \rightarrow \bar{x} = xW/\hbar v_F$, $B \rightarrow \bar{B} = \mu_B B/W$ and $k \rightarrow \bar{k} = \hbar v_F k/W$, where W is the bulk gap, we can rewrite this equation in terms of dimensionless variables as

$$\bar{E}\psi = [-i\sigma_z\partial_{\bar{x}} + \frac{g}{2}\Delta_L(\bar{x})\vec{\sigma}\cdot\vec{\bar{B}}]\psi. \qquad (4)$$

We will henceforth drop the bar's.

Magnetic field twists helicity :- The Hamiltonian given in Eq. (1) describing free edge state electrons is time-reversal-symmetric. But the Zeeman-coupling term H_B in Eq. (2) breaks time-reversal symmetry and opens up a gap in the spectrum. This happens in the region where the magnetic field is nonzero, i.e., $|x| < L/2$. In regions of zero magnetic field we know that up-spin (pointing along $+Z$ direction) moves right and down-spin (pointing along $-Z$ direction) moves left. But in the region with non-zero magnetic field, this is no longer true. However, as we shall see, the direction of motion is still correlated with the spin orientation for propagating states above and below the gap. To look for the eigenstates of the Hamiltonian $H_0 + H_B$ in the region $|x| < L/2$, we start with a plane wave solution $\psi_k e^{i(kx-\omega t)}$ where ψ_k is the Fourier transform of the spinor field $\psi(x)$. Substituting the above form into Eq. (3), we find the dispersion relation to be- $E = \pm\sqrt{\tilde{k}^2 + b_X^2}$, where $b_X = gB_X/2$, $b_z = gB_z/2$ and $\tilde{k} = k + b_z$. Thus, the spectrum is gapped for nonzero B_X with a gap given by b_X and the spectrum breaks into two bands.

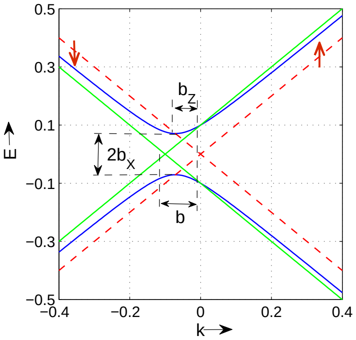

FIG. 2. Blue (dark-solid) and green (light-solid) curves stand for schematic dispersions when the $\vec{B}$-field is at angles $\phi = \pi/4$ and $\phi = 0$ with the positive Z-axis respectively. $b = |\vec{b}| = 0.1$ in both cases. Red (dashed) curve corresponds to the zero field case.

The magnetic field $\vec{B}$ can be in general at an angle ϕ with Z-axis i.e., $\vec{b} = b(\sin\phi\hat{X} + \cos\phi\hat{Z})$. The dispersion relation for the three different cases corresponding to $\vec{b} = 0$ and directions $\phi = 0$ and $\phi = \pi/4$ with non-zero b, is shown in Fig. 2. Note that in the presence of a finite $\vec{B}$ field, the zero momentum state, i.e., $k = 0$ states are split exactly by $2b_X$ as expected for spin half particles with zero momentum.

At a given energy E the there are two eigenstates - right- and left-moving $\psi_{E,R/L}$ with momentum $k = k_R$ and $k = -k_L$ respectively given by -

$$\psi_{E,R} = \frac{1}{N}\Big[E + \tilde{k}_0 \qquad b_X\Big]^T;\ \psi_{E,L} = \sigma_x\psi_{E,R}$$
$$\text{and } k_{R/L} = [\mp b_z + sign(E)\sqrt{E^2 - b_X^2}], \qquad (5)$$

where N is the normalization and $\tilde{k}_0 = (k_R + k_L)/2$. Unlike the free HES, here each state ψ_E has its spin pointing in a distinct direction and the left and right moving modes are no longer anti-parallel. At a given energy E (not in the gap i.e., $|E| < |b_x|$), we find the spin orientation $\vec{S}_P = \langle\ \psi_P\,|\,\vec{S}\,|\,\psi_P\ \rangle$ for the right/left movers ($P = R/L$) where $\vec{S} = \vec{\sigma}/2$ is the spin operator, to be given by $S_{R/L} = (b_x, 0, \pm\tilde{k}_0)/2E$. When $|E| \gg |b_x|$, the spin for the R/L movers point along the $Z/-Z$ direction as expected. Also, note that the states at the bottom of upper band and top of lower band are located at $k = -b_z$ which implies that $\tilde{k}_0 = 0$; here, the respective spins point parallel and anti-parallel to the X-axis. For this value of the momentum, the momentum dependent pseudo-magnetic field acting on the electron due to the helical nature of the free Hamiltonian is fully canceled by the Z component of the applied magnetic field; hence it leaves behind a net $\vec{B}$-field pointing along the X direction [10]. On a more general note, in a given band, if we look at left-moving and right-moving modes with the same energy, the magnetic field component B_x twists them by the same angle, but in opposite directions as sketched in Fig. 1.

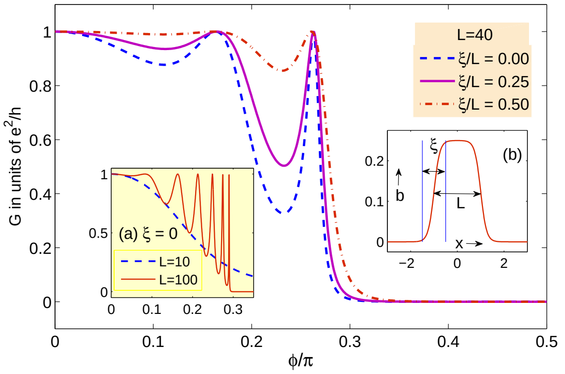

FIG. 3. Main figure: Differential conductance G vs angle ϕ for different ξ/L . Inset(a): G vs ϕ for two different lengths of the patch with $\xi = 0$. Inset(b): Illustration of how $b = |\vec{b}|$ changes across the patch for a fixed ϕ. Parameters- $b_0 = max.\{|\vec{b}|\} = 0.25$ and $E_i = 0.2$ are the same in all the plots.

Transmission through the magnetic patch :- Let us consider the case where an electron is incident on the $\vec{B}$-field patch from the left with an energy E_i and momentum $k_i = E_i$. Then the corresponding left and right moving momentum eigenstates that the incident particle excites in the patch region can be read off from Eq. (5) with $E = E_i$. The scattering states in different regions are given by

$$\psi = \begin{cases} |\uparrow\rangle\, e^{ik_i x} + r_{k_i} |\downarrow\rangle\, e^{-ik_i x} & \text{for } x < -L/2, \\ A_R\, \psi_{E_i\, R}\, e^{ik_R x} + A_L\, \psi_{E_i\, L}\, e^{-ik_L x} & \text{for } |x| < L/2, \\ t_{k_i}\, e^{ik_i x} |\uparrow\rangle & \text{for } x > L/2, \end{cases} \tag{6}$$

where $|\uparrow\rangle$ and $|\downarrow\rangle$ are eigenstates of σ_z, r and t are the reflection and the transmission amplitudes and A_L and A_R are the amplitudes corresponding to the left and right moving eigenstates in the $\vec{B}$-field patch. Using appropriate boundary conditions, one gets the following expression for transmission amplitude-

$$t_{k_i} = \frac{\tilde{k} e^{-i(k_i + b_z)L}}{\tilde{k}\cos[\tilde{k}L] - ik_i \sin[\tilde{k}L]} \,. \tag{7}$$

Note that the resonance corresponds to $(k_R + k_L)L = 2n\pi$ which is the total phase picked up by the electron in one round trip journey across the $\vec{B}$ field patch, *i.e.*, very similar to the double barrier resonance. The crucial difference between the two emerges when we look at the dynamics of the spin in the $\vec{B}$-field patch. This will be addressed below. The most interesting point to note here is the fact that the resonance condition does not depend on $|\vec{B}|$ but only on B_x. Hence the resonances can be tuned simply by rotating the $\vec{B}$-field away or toward the Z-axis without changing its magnitude. This observation is the central message of this letter. A plot of the transmission probability at fixed k_i, which is the differential conductance in units of e^2/h evaluated at fixed bias, corresponding to an electron incident with energy E_i from the left reservoir while the right reservoir is held at zero potential, is shown as a function of ϕ in Fig. 3-inset-a. Here ϕ is the angle the $\vec{B}$-field makes with the Z-axis in the $X - Z$ plane. As we can see from Fig. 3-inset-a the conductance shows sharp resonances as we vary ϕ for $L = 100$. Note that the resonances get sharper as b_x approaches E_i from $b_x = 0$, and beyond E_i, transport is subgapped. On the other hand note that for a short $\vec{B}$-field patch, ($L = 10$ in Fig. 3-inset-a), the transport is non-resonant, but the differential conductance can be as large as $0.1\ e^2/h$ in the subgapped regime ($\phi > 0.3\pi$). Further, we have studied these resonances for a more realistic $\vec{B}$-field patch wherein magnetic field changes from zero to maximum smoothly over a length-scale ξ as illustrated in Fig. 3-inset-b. We see from Fig. 3 that the visibility of the resonances is affected by increasing ξ. However, even the least visible first resonance (around $\phi = 0.18\pi$), which is most affected by increasing ξ is still visible for ξ in the range $(0, 0.25)$.

Spin orientation in the magnetic patch :- In the presence of a magnetic field, the kinetic energy term competes with the Zeeman term and as a result, the left and right movers point in different directions. (see Eq. (5)). Hence when an electron is incident from the left on the $\vec{B}$-field patch, its spin is expected to precess as it undergoes multiple reflections inside the magnetic field patch due to the mismatch of the spin orientation of the incident electron and the spin orientations of the right and left moving modes present inside the patch. But at resonance, the vanishing of the reflection amplitude for the incident electron exactly amounts to an integer number of complete spin precessions of the electron wave inside the magnetic field patch. Thus, at resonance, the incident spin rotates back to its original orientation at the end of its journey inside the patch. We will show below that the precession dynamics in the $\vec{B}$-field patch is unconventional and carries nontrivial signatures of the spin anisotropy of the HES. We first start by computing the spin orientation at each point x between $x = -L/2$ and $x = L/2$ using the wave-functions given in Eq. (6). Note that since the wave function in the region of magnetic field is a linear combination of left-moving and right-moving eigenstates,

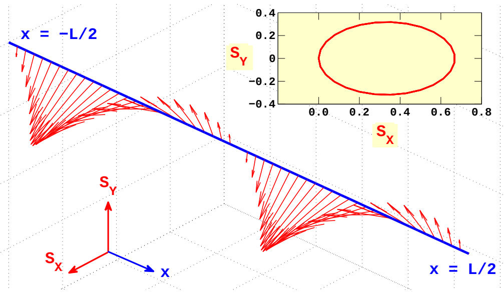

FIG. 4. X and Y components of spin-density at different points in the magnetic-patch for resonant transport $b_{_X} = 0.1, b_{_Z} = 0, L = 180, k = 0.0366$. The inset shows $S_{_X}$ and $S_{_Y}$ at different values of x, $S_{_Y} = 0$ at $x = -L/2, -L/4, 0, L/4, L/2$ while $S_{_X} = 0$ at $x = -L/2, 0, L/2$.

the spin at any given x can, in general, point out of the $X-Z$ plane even though the left and right moving eigenstates are restricted to the $X-Z$ plane. Hence evaluating $\langle\, \psi \,|\, \vec{\sigma}/2 \,|\, \psi \,\rangle$ for the $\vec{B}$-field patch using the wavefunctions given in Eq. (6) corresponding to an electron incident from the left with momentum k_i, we find

$$\langle\, \vec{S}_{k_i}(x) \,\rangle = \frac{1}{2}\frac{1}{\tilde{k}^2 + b_{_X}^2 \sin^2(\theta/2)} \cdot \\ \left(b_{_X} k_i[1-\cos(\tilde{\theta})], -2\,\tilde{k}\, b_{_X} \sin\tilde{\theta}, \tilde{k}^2\right) \,, \quad (8)$$

where $\tilde{\theta} = (x/L-1/2)\theta$ and $\theta = 2\,\tilde{k}\,L$. It can be seen that as x is changed from $-L/2$ to $L/2$, the $S_{_Z}$-component remains unaltered while the $S_{_X}$ and $S_{_Y}$ components trace out the locus of an ellipse.Moreover, the spin density $\vec{S}_k(x)$ at any point x makes a constant angle with the axis $\vec{n}_k = (b_{_X}, 0, k) \cdot 1/\sqrt{k^2 + b_{_X}^2}$. Hence by analogy to the case of precession of the spin of a static spin-half particle in a magnetic field, we see that $\vec{n}_k$ defines the direction of the effective magnetic field around which the spin density precesses as a function of x as we move along the $\vec{B}$-field patch. Note that this precession is quite novel in the sense that the component of the spin vector along the precession axis $\vec{n}_k$ varies as the spin precesses, whereas the component along the Z-axis is preserved. This is distinct from the usual case where the component along the precession axis is preserved. The elliptical shape of the $X-Y$ projection of the precession is a mere reflection of the fact that the Z-axis is not the same as the precession axis. Finally, note that for the resonant case, $\theta = 2n\pi$ at $x = \pm L/2$. This implies that $\tilde{\theta}$ is also $2n\pi$, and hence, $\vec{S}_{k_i} = \hat{Z}/2$ (see Eq. (8)) at both $L/2$ and $-L/2$. This implies that the angle of precession of the electron in the resonant case is an exact integer multiple of 2π which is very similar in spirit to the operational principle of the Datta-Das transistor [11]. Note that even for any finite transmission $\vec{S}_{k_i}$ must always point along $\hat{Z}$ for $x \geq L/2$. But if there is finite reflection at $x = -L/2$ then the spin for $x \leq -L/2$ definitely points away from $\hat{Z}$ as the reflected wave always populates spin down states due to the helical nature of the edge states. So it is clear that for finite reflection, the direction of $\vec{S}_{k_i}$ at $x = -L/2$ can never be the same as that of $x = L/2$. Thus, the resonance condition is directly coupled to evolution of spin density along the $\vec{B}$-field patch. This implies that our set-up can be regarded as a possible candidate for devising a spin-transistor.

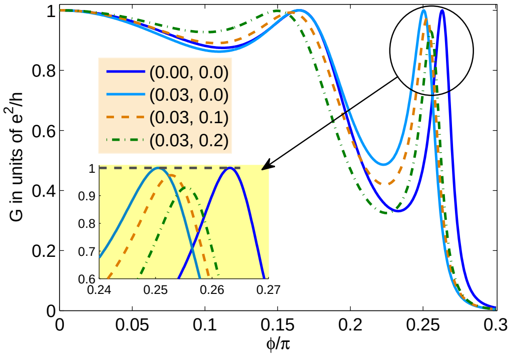

FIG. 5. Illustration of change in visibility of resonances due to disorder of strength $\eta = 0.03$ in the patch. Parameters chosen are same as that in Fig. 3 except $\xi/L = 0.05$, $l/L = 0.1$. The legend shows $(\eta, x_l/L)$ for different curves.

Conditions for experimental observation:- (i) The ratio ξ/L has to be small. $\xi/L < 0.25$ would be a reasonable limit for a typical case as mentioned earlier. (ii) The magnetic field that opens up a gap in the spectrum should not force the edge states to tunnel into the bulk. This means that the gap opened on the edge by $\vec{B}-$field should be less than bulk gap ($2|b_{_X}| < 1$) and the energy of the incident electron should also be within the bulk gap ($|E_i| < 1/2$). A limit on the magnetic field then can be estimated to be 7 Tesla [15]. (iii) Disorder: The topological protection against back-scattering due to scalar impurities breaks down in the presence of the time-reversal breaking magnetic field. Hence one cannot naively throw away the disorder term. In a good sample we expect the disorder to be weak, sparsely spaced and to have a length-scale $l \ll L$. Such an impurity can be modelled by a rectangular potential-barrier/well with width l and height η. This impurity may be centered anywhere ($|x_l| < L/2$) in the magnetic field patch. We have studied the effect of such an impurity with a fixed l with different disorder-strengths η, positioned across the patch ($|x_l| < L/2$). We find that as long as $|\eta| \ll |E_i|$ the resonances are not affected. We have given an illustrative plot in Fig. 5 of how the resonances are affected for a value of $\eta/E_i = 0.15$ positioned in the patch [16].

Discussion and conclusion:- The most crucial element involved in devising the proposed set up is to realize the localized $\vec{B}$-field patch whose direction should be fully tunable. It should be possible to engineer such a localized $\vec{B}$-field patch using the proximity effect [13] by depositing a layer of magnetic material on top of the edge. Moreover, by choosing a magnetic material which shows current induced rotation of magnetization [12], it should be possible to rotate the direction of the $\vec{B}$-field in the patch. So in conclusion, we have discussed a concrete proposal to probe the degree of spin anisotropy in the HES via the Fabry-Pérot resonances. Note that similar surface states appear in 3-D topological insulators and the extent to which such states are helical (spin-momentum locked) is not yet fully understood. Also, these have been probed not via direct transport experiments but via optics experiments such as spin-resolved ARPES which see a deviation[14] from the purely theoretical picture of the 2-D helical states. Hence in the context of 2-D topological insulators where 1-D HES appear on the boundary, studying these resonances could lead to crucial information and characterization of deviations from the theoretically predicted helical nature, if any. Also as an application, our set-up provides a possible design for a resonant spin transistor.

Acknowledgments .- We thank Diptiman Sen, Amir Yacoby and Yuval Oreg for stimulating discussions. A.S. thanks HRI and DU, for kind hospitality during the stay and CSIR, India for financial support. S.R. thanks ICTS, Bangalore for kind hospitality during the completion of this work.

---

[1] C. L. Kane and E. J. Mele, Phys. Rev. Lett. **95**, 226801 (1995); ibid, Phys. Rev. Lett. **95**, 146802 (2006); M. Buttiker, Science **325**, 278 (2009); M. Z. Hasan and C. L. Kane (2010), arXiv:1002.3895; Xiao-Liang Qi and Shou-Cheng Zhang, Rev. Mod. Phys. **83**, 1057 (2011).

[2] C. Wu, B. A. Bernevig, and S. C. Zhang, Phys. Rev. Lett. **96**, 106401 (2006); C. -Y. Hou, E. -A. Kim, and C. Chamon, Phys. Rev. Lett. **102**, 076602 (2009) ; J. Maciejko, C. Liu, Y. Oreg, X. -L. Qi, C. Wu, and S. C. Zhang, Phys. Rev. Lett.**102**, 256803 (2009) ; A. Ström and H. Johannesson, Phys. Rev. Lett. **102**, 096806 (2009) ; A. Bermudez, D. Patane, L. Amico, M. A. Martin-Delgado, Phys. Rev. Lett. 102, 135702 (2009) ; J. E. Moore, Nature **464**, 194 (2010); N. Goldman, I. Satija, P. Nikolic, A. Bermudez, M. A. Martin-Delgado, M. Lewenstein, I. B. Spielman, Phys. Rev. Lett. 105, 255302 (2010) ; R. Egger, A. Zazunov and A. Levy Yeyati, Phys. Rev. Lett. **105**, 136403; P. Virtanen and P. Recher, Phys. Rev. **B 83**, 115322 (2011).

[3] M. Konig et al., Science **318**, 766 (2007); M. Konig et. al., J. Phys. Soc. Japan, (2008).

[4] Joseph Maciejko, Eun-Ah Kim and Xiao-Liang Qi, Phys. Rev. B **82**, 195409 (2010).

[5] Jan Carl Budich , Fabrizio Dolcini , Patrik Recher, and Bjorn Trauzettel, arXiv:1109.5188 (unpublished).

[6] A. V. Parafilo et al., Low temp. Phys., **36**, 959 (2010); A. V. Parafilo et al., Phys. Rev B **83**, 045427 (2011).

[7] S. Mondal, D. Sen, K. Sengupta, and R. Shankar, Phys. Rev. Lett. **104**, 046403 (2010).

[8] S. Das and S. Rao, Phys. Rev. Lett. **106**, 236403 (2011); K. Saha, S. Das, K. Sengupta and D. Sen, Phys. Rev. **B 84**, 165439 (2011).

[9] C. Brune et al, Nature Physics **8**, 485 (2012).

[10] Maxim Kharitonov, arXiv:1004.0194 (unpublished).

[11] S. Datta and B. Das, Appl. Phys. Lett. **56**, 665 (1990).

[12] V. Uhlir et al, J. Phys. Cond. Mat., 24(2), 024213 (2012).

[13] R. J. Epstein, et al, Phys. Rev. **B 65**, 121202(R) (2002).

[14] Z.-H. Pan et al., Phys. Rev. Lett. 106, 257004 (2011).

[15] For HgTe, $g \sim 50$ (M.V. Yakunin et al., Physica E, **42**, 948 (2010)) and $\mathrm{bulk-gap} \sim 0.02eV$ (RMP in Ref. [1]).

[16] A more detailed analysis of disorder is under preparation.